JREE: Vol. 10, No. 2, (Spring 2023) 9-18

Journal of Renewable Energy and Environment

Journal Homepage: www.jree.ir

Materials and Energy Research Center

MERC

Research Article

Optimal Location and Sizing of Wind Turbines and Photovoltaic Cells in the Grid for Load Supply Using Improved Genetic Algorithm

Ming Hung Lin [a], Jiun Hung Lin [b], Mamdouh El Haj Assad [c*], Reza Alayi [d,e*], Seyed Reza Seyednouri [f]

[a] *Department of Electrical Engineering, Cheng Shiu University, 83347, Kaohsiung City, Taiwan, China.*
[b] *College of Electrical Engineering and Computer Science, National Kaohsiung University of Science and Technology, 811, Kaohsiung City, Taiwan, China.*
[c] *Department of Sustainable and Renewable Energy Engineering, University of Sharjah, P. O. Box: 27272, Sharjah, United Arab Emirates.*
[d] *Department of Mechanics, Germi Branch, Islamic Azad University, P. O. Box: 5651763764, Germi, Ardabil, Iran.*
[e] *Energy Research Center, Shahrekord Branch, Islamic Azad University, Shahrekord, Chaharmahal and Bakhtiari, Iran.*
[f] *Young Researchers and Elite Club, Germi Branch, Islamic Azad University, P. O. Box: 5651763764, Germi, Ardabil, Iran.*

PAPER INFO

Paper History:
Received: 30 January 2022
Revised: 19 June 2022
Accepted: 23 June 2022

Keywords:
Optimal Placement,
Improved Genetic Algorithm,
Distributed Production,
Loss Reduction,
Combined System

ABSTRACT

The optimal combination of distributed generation units in recent years has been designed to improve the reliability of distributed generation systems as well as to reduce losses in electrical distribution systems. In this research, the improved Genetic Algorithm has been proposed as a powerful optimization algorithm for optimizing problem variables. The objective function of this paper includes power loss reduction, hybrid system reliability, voltage profile, optimal size of distributed generation unit, and finally improvement of the construction cost of combined wind and solar power plants. Therefore, the problem variables are subject to reliable load supply and the lowest possible cost during the optimization process. In order to achieve this goal in this study, the IEEE standard 30-bus network is examined. The results of the system simulation show the reduction of total system losses after DG installation compared to the state without DG and the improvement of other variable values in this network. This loss index after installing DG in the desired bus has a reduction of about 200 kWh during the year and has a value equal to 126.42 kWh per year.

https://doi.org/10.30501/jree.2022.327250.1321

1. INTRODUCTION

Studies have shown that more than 70 % of the total power system losses are related to distribution networks, being more than 13 % of the total production capacity [1-3]. These electrical losses can be reduced by installing and controlling dispersed production devices. The use of distributed generation is widely used in distribution networks, the advantages of which include voltage regulation, loss reduction, power factor correction, and system capacity liberalization [4-6]. In order to determine the location, number, size, type, and control plan of distributed generation over a period of one to ten years, a complex optimization problem with conflicting objectives such as minimizing the cost of purchasing and installing distributed generation and reducing electrical losses can be addressed [7-9]. Since the 1960s, several methods have been proposed in this field. These methods can be divided into four groups: analytical, numerical programming, innovative methods, and artificial intelligence methods. Most of the research studies presented in this field have not considered a number of important aspects such as considering distributed generation in a discrete way with real prices and quantities available in the market [10-12], considering unbalanced load and network [13-15], presence of harmonic currents and voltages due to extensive use of harmonic generating loads and electronic power devices [16-18], reaction and coupling between harmonic voltages and currents created by nonlinear loads [19-21], increase of harmonic currents due to intensification [22-24], and IEEE power quality constraints [25, 26]. Power plants are used as distributed generation in distribution networks.

The main purpose of this research is to determine the location and optimal capacity of distributed generation units by considering these five objectives: reducing losses, improving voltage profile, improving system reliability, the optimal size of DG unit, and reducing the construction cost of combined wind and solar power plants. Each of these individual goals has been transformed into a single-objective function using weighting coefficients. These coefficients are determined using the AHP method and applied to the objective function of the problem.

2. MATERIAL AND METHOD

*Corresponding Authors' Email: massad@sharjah.ac.ae (M. El Haj Assad) and reza_alayi@iaugermi.ac.ir (R. Alayi)
URL: https://www.jree.ir/article_155023.html

Please cite this article as: Lin, M.H., Lin, J.H., El Haj Assad, M., Alayi, R. and Seyednouri, S.R., "Optimal location and sizing of wind turbines and photovoltaic cells in the grid for load supply using improved genetic algorithm", ***Journal of Renewable Energy and Environment (JREE)***, Vol. 10, No. 2, (2023), 9-18. (https://doi.org/10.30501/jree.2022.327250.1321).

2.1. Case study

The intermittent behavior of the intensity of solar radiation has caused solar power plants to not have continuous and controllable characteristics. Wind power plants also do not have a uniform characteristic due to intermittent wind intensity. In this paper, in order to achieve uniform energy from renewable sources, a combination of wind and solar units is used. From the point of view of the power system, a solar power plant, which can include several photovoltaic panels with different capacities, is one of the sources of uncertainty in the system. In system studies in the presence of wind and solar power plants, their output power must first be determined. The output power of the combined wind and solar power plant depends on the intensity of the sun radiation and the intensity of the wind in the installation area. Therefore, the intensity of sunlight and wind in the study area must be calculated and then, the solar and wind panel model must be determined. The studies of this paper are based on the data of solar radiation intensity and wind, which are the daily average of the New Energy Organization of Iran (SANA) for the Meshkinshahr region located in northwestern Iran, and the data has been applied in system simulation. Graphs related to the intensity of solar radiation and wind intensity in the study area can be seen in Figures 1 and 2, respectively.

Among the important issues that should be considered in the optimal placement of distributed generation sources in the distribution network is the existence of an unbalanced network and load and the effect of nonlinear and harmonic loads. Such network load is unbalanced. Therefore, it is necessary to optimize the house by considering the unbalanced load condition. This issue has not been considered in most of the research methods.

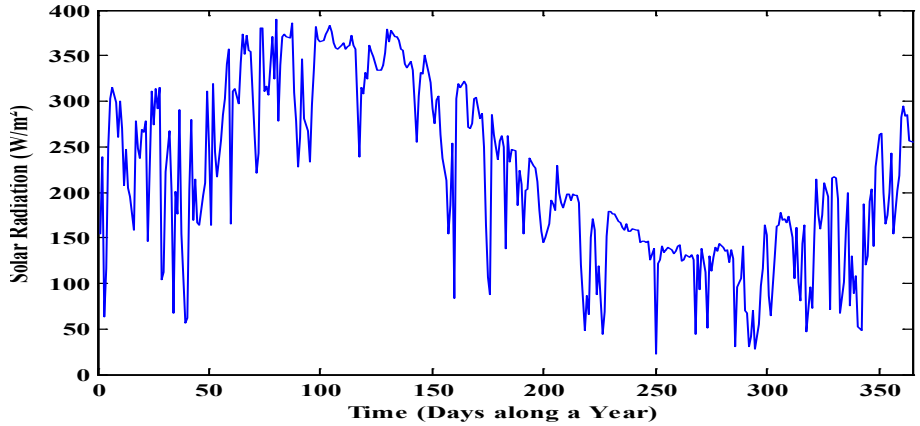

Figure 1. Intensity of solar radiation throughout the year for Meshginshahr

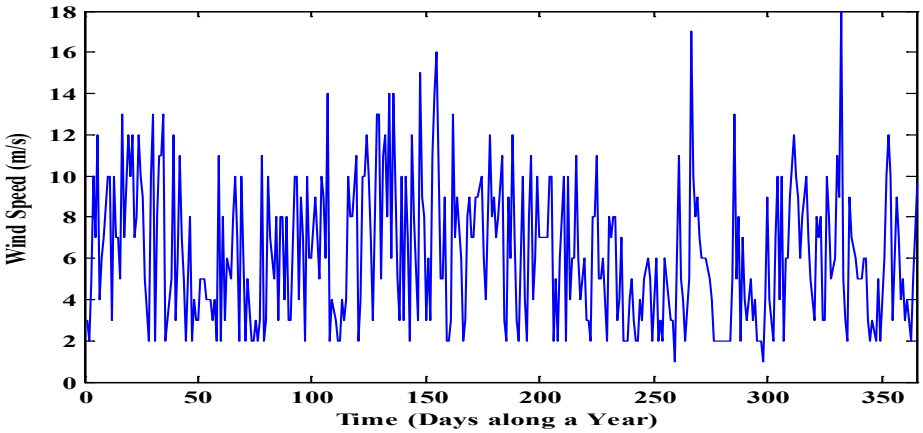

Figure 2. Intensity of wind speed throughout the year for Meshginshahr

2.2. System model in harmonic frequencies

At harmonic frequencies, accurate models are available for distribution lines and parallel capacitors. However, the exact harmonic model of the power supply system, distribution lines, transformer stations, and linearity and non-linearity is not available. If the skin effect is ignored, the capacitor and the lines can be shown as follows in the n^{th} harmonic [27, 28].

$$y_c^n = n y_c^1 \quad (1)$$

$$y_{i,i+1}^n = (R_{i,i+1} + jnX_{i,i+1}) \quad (2)$$

where $R_{i,i+1}$ and $X_{i,i+1}$ show the values of the position and reactance of the line between the i and i + 1 buses, respectively. Power sources and transformers are usually denoted by short-circuit admittances, y_c^n and y_c^1, and entering the scale of harmonics. With respect to linear loads, a general resistance model parallel to the inductor is used to show the active and reactive powers at the main frequency. If only (w_i-1) which is the share of linear loads in the ith bus is assumed, the load admittance at the kth level is expressed as follows:

$$y_a^n = \frac{1 - w_i}{|V_a^2|}\left(P_a - j\frac{Q_a}{n}\right) \quad (3)$$

Nonlinear loads are also usually considered as ideal current sources. Composite loads are modeled as an impedance (linear load share) parallel to a current source (nonlinear load share). It should be noted that under harmonic conditions, there are negative and zero sequence components of the current even in the balanced networks. In addition, the multiples of three all appear in zero sequences; thus, a fundamental factor in voltages and multiples includes a three-fold approach connecting capacitive banks, transformers, and loads.

2.3. Network modeling in the presence of harmonics

The distribution network is modeled by considering the harmonic in the form of a single-line diagram shown in Figure 3. The distribution of the harmonic load after modeling the system is described below.

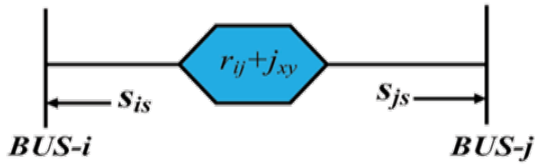

Figure 3. Single-line diagram of a feeder in a distribution network

Modeling a feeder is done according to the following steps:

1) The amplitude and angle of the voltage phase of each bus are obtained using the Backward/Forward Sweep Power Flow Method and based on the results, the resulting network losses are calculated.

2) At high frequencies, the power system is modeled as a combination of current sources and passive elements, because the admittance of system components changes with a harmonic order change. The admittance matrix must be modified in each harmonic order.

3) Linear loads are modeled as resistance and parallel reactance. Nonlinear loads are considered as current sources; thus, the harmonic current injected by the nonlinear loads in the ith bus is calculated according to Equation (4), and the index $C(h)$ in each harmonic order is based on Fourier analysis.

$$\begin{bmatrix} V_1^k \\ V_2^k \\ \vdots \\ V_{n-1}^k \\ V_n^k \end{bmatrix} = \begin{bmatrix} Y_{11}^k & Y_{12}^k & 0 & & \\ Y_{21}^k & Y_{22}^k & \vdots & & \\ \vdots & & & & \\ & & Y_{m-1m-1}^k & & Y_{m-1\,m}^k \\ 0 & 0 & Y_{mm-1}^k & & Y_{mm}^k \end{bmatrix}^{-1} \begin{bmatrix} I_1^k \\ I_2^k \\ \vdots \\ I_{n-1}^k \\ I_n^k \end{bmatrix} \quad (4)$$

$$I_i^I = \left[\frac{P_{hi} + jQ_{hi}}{V_{iI}}\right]^n \quad (5)$$

$$I_i^h = C(h) I_i^I \quad (6)$$

4) The effective value of voltage at bus i is calculated by Equation 7 as follows:

$$|V_i| = \sqrt{\sum_{h=1}^{H} |V_i|^2} \quad (7)$$

where P_i and Q_i are the active and reactive power of the 1st load in the 1st bus, respectively. R and X are the resistance and reactance between successive buses i and i + 1, respectively, and H is the highest harmonic order.

2.4. Power losses

Power loss is considered as one of the important goals in studies related to distributed generation. It is considered as the most important single goal and is stated as follows:

$$P_{L_{total}} = \sum_{i=1}^{n} R_i I_i^2 \quad (8)$$

$$F_1 = \frac{P_{loss,i}}{P_{loss,base}} \quad (9)$$

where I_i is the current passing through line i, n is the total number of lines, and R is the resistance of line i. $P_{loss,i}$ is the P_{loss} value for the ith branch after DG installation and $P_{loss,base}$ is the initial value of P_{loss}.

2.5. System reliability

To show a more tangible view of the overall network status, system-related reliability indicators are used to show the behavior of the entire feeder. Some of these indicators that are used in this work are:

- The system average interruption frequency index (SAIFI):

$$SAIFI = \frac{\sum \lambda_i . N_i}{\sum N_i} \quad (10)$$

where λ_i is the failure rate and N_i is the number of customers for location i.

- The System Average Interruption Duration Index (SAIDI):

$$SAIDI = \frac{\sum_{i=1}^{n} U_i . N_i}{\sum_{i=1}^{n} N_i} \quad (11)$$

In the above relation, U_i is the annual outage time for location i (h/year).

- The Average Energy Not Supplied (AENS):

$$AENS = \frac{ENS}{\sum N_i} \quad (12)$$

In the above relation, ENS is the Energy Not Supplied in terms of (kWh/year). The general system reliability index is examined through the following equation:

$$F_2 = \left[\left(\frac{SAIFI_i}{SAIFI_{base}}\right) + \left(\frac{SAIDI_i}{SAIDI_{base}}\right) + \left(\frac{AENS_i}{AENS_{base}}\right)\right] \quad (13)$$

where $SAIFI_i$ is the system average interruption frequency index after DG installation and $SAIFI_{base}$ is the system average interruption frequency index for the primary network without DG installation. The other indicators of the above relationship are the same.

2.6. The optimal size of DG

The optimal size of the DG can be calculated by the following index:

$$F_3 = \frac{P_{DG_{i,j}}}{\sum_{j=1}^{N_P} P_{load_j}} \quad (14)$$

where $P_{DG_{i,j}}$ is the power on the bus j for the ith branch, P_{load_j} is the active power of the load point j, and N_P is the total number of load points.

2.7. Network voltage profile

The function F_4 is the voltage profile index and is calculated as follows:

$$F_4 = \sum_{i=1}^{n} (1 - |V_i|)^2 \quad (15)$$

In the above relation, V_i is the bus voltage at point j.

2.8. Cost of operating the hybrid system

The function F_5 is the index for the total cost of the wind and solar hybrid system, which is calculated by the following equation [29, 30]:

$$F_5 = \left(\frac{C_{DG}}{C_{DG_T}}\right) \quad (16)$$

$$C_{DG} = \sum_S NPC(S) = N \times (CapitalCost + (Re\,placementCost \times k)) + (O\&MCost \times \frac{1}{CRF(ir,\pi)}) \quad (17)$$

where the vector S is equal to $C_{DG,\,s}$ = (PV + WT) which is the base cost. In this case, it is equal to C_{DGT} = 1000000. CRF is the capital recovery factor that is calculated by the following equation [29, 30]:

$$CRF(ir, R) = \frac{ir(1+ir)^R}{(1+ir)^R - 1} \quad (18)$$

where ir is the discount rate and R is the project lifetime.

2.9. Modeling of the studied equipment

2.9.1. Photovoltaic system

The output power of photovoltaic panels can be calculated using Equations (19) to (21). This model includes the effects of solar radiation and panel temperature on its output power. These relationships at the maximum output power point are as follows [4, 9]:

$$P_{PV} = V_{MPP}.I_{MPP} \quad (19)$$

$$V_{MPP} = V_{MPP,ref} + P_{v,oc}(T_C - T_{C,ref}) \quad (20)$$

$$(I_{MPP} = I_{MPP,ref} + I_{SC,ref}(\frac{G_T}{G_{ref}}) + P_{I,SC}(T_C - T_{C,ref}) \quad (21)$$

where P_{PV} is the panel power, V_{mpp} is the potential voltage, $V_{mpp,\,ref}$ is the same as V_{mpp} in standard operating conditions (V), I_{mpp} is the panel current, $I_{SC,\,ref}$ is the short circuit current in standard operating conditions, G_T is the average daily radiation (W/m^2), and G_{ref} is equivalent to 1000 W/m^2 for operation under standard conditions. $P_{V,\,oc,}$ and $P_{I,\,SC}$ are the temperature coefficients for open-circuit voltage (V/°C) and short circuit current (A/°C), respectively. $T_{C,ref}$ is the temperature of the photovoltaic panel under standard operating conditions, which is considered to be 25 °C, and T_C (t) is the operating temperature of the photovoltaic panel, which is calculated as follows:

$$T_C(t) = T_a(t) + \frac{NOCT - 20}{800}.G_T \quad (22)$$

where $T_a(t)$ is the ambient temperature (°C), NOCT (Nominal Operating Cell Temperature) is defined for the operation of the irradiated panel at 800 W/m^2 and a temperature of 20 °C and is usually considered between 40 °C and 46 °C.

Photovoltaic panels in series are defined using DC bus voltage and the nominal voltage of the panel as:

$$N_{PN,S} = \frac{V_{Bus}}{N_{pv,nom}} \quad (23)$$

where $N_{pv,nom}$ is the nominal voltage of the photovoltaic panel. It should be noted that $N_{PN,S}$ is not an optimized target and the number of connected panels in parallel is the optimized targets.

2.9.2. Wind turbine

The wind speed at the reference height h_r is used as the daily average to determine the wind speed colliding with the wind turbine in the model below. The wind turbine model is described as follows:

$$V(t) = V_r(t).\left(\frac{h}{h_r}\right)^{\gamma} \quad (24)$$

where $V(t)$ is the wind speed at height h, Vr is the wind speed recorded at height h, and γ is called the legal power view, which is between 0.14 and 0.25. This formula of wind speed calculation is used to calculate the turbine output power P_{WT} (t) as follows [4, 9]:

$$P_{WT}(t) = \begin{cases} av^3(t) - bP_R & V_{C_i} < V < V_r \\ P_R & V_r < V < V_{CO} \\ 0 & \text{otherwise} \end{cases}$$
$$b = \frac{V_{Ci}^3}{(V_r^3 - V_{Ci}^3)}, a = \frac{P_r}{(V_r^3 - V_{Ci}^3)} \quad (25)$$

where P_r is the allowable power. V_{co}, V_r, and V_{Ci} are the low cut-off speed, nominal speed, and high cut-off speed of the turbine, respectively.

2.9.3. DC/AC converter

The DC/AC converter is used to convert the total DC power from the hybrid power plant into AC power at the desired frequency. In order to investigate the converter losses on the output power of the hybrid power plant, the following equation is used:

$$P_{inv-load} = (P_{Re\,n-inv}) \times \eta_{inv} \quad (26)$$

where η_{inv} is the converter efficiency. Costs related to investment, maintenance, replacement of parts, and operating costs of the system are shown in actual values in Table 1.

Table 1. Technical specifications of the used equipment

Equipment	Investment cost ($/unit)	Replacement cost ($/unit)	Annual fee (Repair and maintenance) ($/unit-yr)	Life-time (yr)	Accessibility (%)	Efficiency (%)
PV	7000	6000	20	20	96	--
WG	19400	15000	75	20	96	--
DC/AC	800	750	8	15	99/89	90

2.10. Optimization

2.10.1. Improved GA algorithm

Considering the advantages and disadvantages of each of the real and binary coding methods and considering that there are both continuous and discrete variables in the problem of optimal placement of scattered products, the proposed genetic algorithm uses the combined coding method. In this coding method, each chromosome is divided into two parts: continuous variables and discrete variables. This coding method significantly reduces the length of the string and reduces the computational volume. Moreover, in this method, it is possible to use the advantages of both real and binary coding methods and no approximation is required to execute the obtained answer.

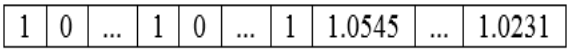

Figure 4. String structure

2.10.2. Genetic operators

Since in the proposed genetic algorithm, each chromosome is divided into two parts, continuous and discrete, it is necessary to define the genetic operators of mating and mutation in accordance with this coding.

2.10.3. Coupling

The genetic operator function selects the length of the binary and real parts of the operators proportional to the selected strings as the parent. The advantage of this method is that operators that respond better to continuous variables can be used for the real part while operators that work better for discrete variables can be used for the binary part. The mating operator presented in this dissertation is a scattered-exploration operator. This operator uses the scattered operator for the binary part and the more efficient exploration operator for the real part. The sparse operator first generates a random string of zeros and ones along the binary portion of the chromosome and then, replaces one of the corresponding genes of the first parent and zero of the corresponding genes of the second parent. The exploration operator generates a point from the pairing of the parent points that is on the line connecting these two points and closer to the better parent. If we assume that parent one is better than parent two, the resulting child will be as follows:

$$\text{Child} = R \times (\text{Parent 2} - \text{Parent 1})$$

where R is the ratio of the child to the better parent. The following figure shows how the sporadic genetic operator works and generates a new string of selected parents.

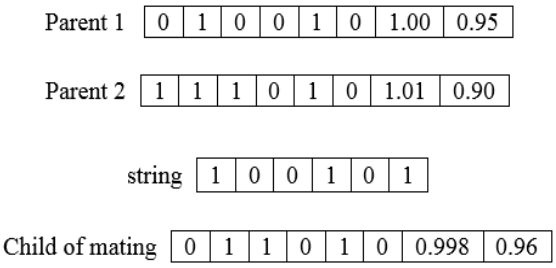

Figure 5. Scattered-exploration operator mutation

The mutation operator for the proposed method first generates a random string of zeros and ones in which the probability of one is equal to the probability defined for the mutation operator. Then in genes corresponding to one, if they are in the binary part, it converts zero to one and one to zero, and if it is in the real part, it puts a random number in the allowable range for that variable instead of the corresponding number. The function of the mutation operator can be seen in the figure below.

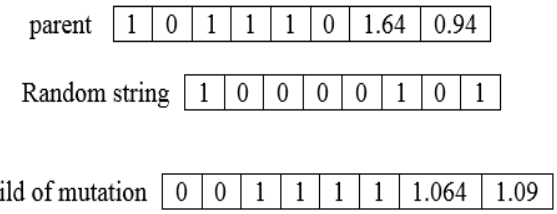

Figure 6. Mutation operator

Execution steps of GA-improved algorithm:

1) Obtain the value of t = 1

2) Produce x chromosome randomly in the desired range

3) Determine the fitness value of the function f (x) and assign this variable value as the best child (x_{best})

4) Calculate the child of the new generation using Equation (1)

5) Take the value $t = t_{max}$

6) Check the condition of completion of steps and determine $x_{optimal}$ based on the following command:

$$\text{If } t=t_{max} \text{ go to step(2) else } x_{optimal}= x_{best}$$

7) The end

Figure 7 shows the GA-improved algorithm process.

2.10.4. Optimal placement of distributed generation

In this section, the objective function of the problem of optimal placement of distributed generation with equal and

unequal constraints is expressed. In this formulation, the effect of harmonic distortion of voltage sources on the network is considered.

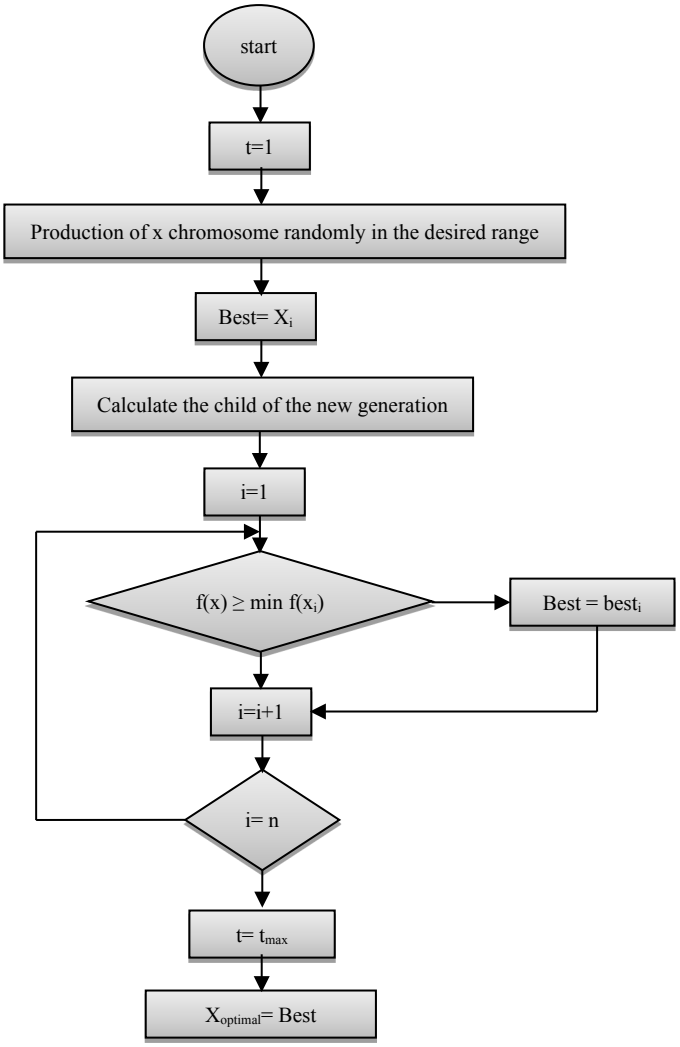

Figure 7. GA-Improved algorithm flowchart

The main purpose of this research is to determine the optimal location and capacity of distributed generation units by considering the five objectives of reducing losses, improving voltage profile, improving system reliability, the optimal size of DG unit, and construction cost of combined wind and solar power plant. Each of these individual goals has been transformed into a single-objective function using weighting coefficients. These coefficients are determined using the AHP method and applied to the objective function of the problem. The AHP model was first used by Thomas L. Saaty in the 1970s. AHP is a simple computational method based on the main operation on the matrix, which calculates its specific values by creating a suitable hierarchy and processing step by step and constructing adaptive matrices at different levels, and in the vector of final weight coefficients, the relative importance of each option is determined according to the purpose of the hierarchy. The first step in calculating weighting coefficients is to prioritize the problem criteria. These values are applied as five priorities in this research in the following relation.

The criteria and sub-criteria used to evaluate sustainable energy options are summarized in the conceptual model shown in Figure 8.

The statistical population of this research dwell in Meshkinshahr. After determination of the potential of renewable energy and economic analysis, the level of prevention of environmental pollutants in comparison is determined with fossil resources. Then, using the analytical network process (ANP) for each of the sub-indicators of the economic dimension, the environmental dimension is assigned to each of the weighted renewable energies. Using the multi-criteria decision method of PROMETHEE, renewable energy (solar, wind) is used from the economic viewpoint and the environmental dimension is scored. Also, free R programming software is used for data analysis, which is an implementation of the ANP weighting method. The ANP method, which is a generalization of the Analytic Hierarchy Process (AHP) method, does not require a hierarchical structure and, therefore, shows the relationship between different levels of a decision in a network.

The preference linear function p (d) is considered and a net superiority value Φ (·) is obtained. The linear function p(d) is obtained as follows:

$$p(d) = \begin{cases} 0 & d \le 0 \\ d/p & 0 \le d \le p \\ 1 & d > p \end{cases} \quad (27)$$

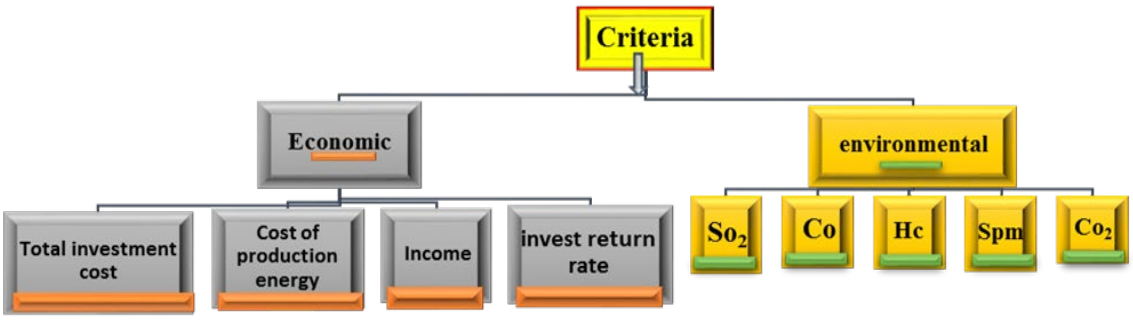

Figure 8. Conceptual model of influential factors of renewable energy

The net superiority value for region a, Φ (a) is calculated as follows:

$$\Phi(a) = \Phi^{+}(a) - \Phi^{-}(a) \quad (28)$$

$$\Phi^{+}(a) = \frac{1}{n-1}\sum_{x \in A} \pi(a,x), \quad (29)$$

$$\Phi^{-}(a) = \frac{1}{n-1}\sum_{x \in A} \pi(x,a), \quad (30)$$

And

$$\pi(a,x) = \sum_{j=1}^{6} p_j(a,x)\, w_j, \tag{31}$$

$$\pi(x,a) = \sum_{j=1}^{6} p_j(x,a)\, w_j, \tag{32}$$

and w_j's are the weights assigned by the AHP method to each of the indicators of urban prosperity in terms of infrastructure. Now, if Φ (b) < Φ (a), region a has less urban flourishing than region b, and vice versa.

Also, to make it easier to interpret the values of superiority between -1 and 1, it can be converted into a score between 0 and 100 using the following conversion:

$$\Phi'(a) = \frac{\Phi^{+}(a) + (1 - \Phi^{-}(a))}{2} \times 100 \tag{33}$$

According to the score presented by Equation (30), the status of operation of five types of renewable energy in Meshkinshahar studied is classified into (0-1) as:

$$A = \begin{bmatrix} W_1/W_1 \dots W_1/W_5 \\ \dots\dots\dots \\ W_5/W_1 \dots W_n/W_5 \end{bmatrix} \begin{bmatrix} W_1 \\ \dots \\ W_5 \end{bmatrix} \tag{34}$$

In the second step, the compatibility coefficient is calculated by the following equation:

$$CR = \frac{CI}{RI} \tag{35}$$

In the above equation, RI is random index and CI is obtained using the following relation:

$$CI = \frac{L - N}{N - 1} \tag{36}$$

$$L = \frac{1}{N}\left(\sum_{i}^{N} = \left(\frac{WA_i}{W_i}\right)\right) \tag{37}$$

According to the above relations, the value of weighting coefficients in this problem is calculated according to the preference and the order of importance is equal to W_1=0.388, W_2=0.2186, W_3=0.1943, W_4=0.1564, and W_5=0.043. In general, the objective function of the problem is to minimize the following equation:

$$\min \quad F = F = \sum_{m=1}^{5} w_m \cdot F_m$$
$$w_m \in [0,1] \qquad \sum_{m=1}^{5} w_m = 1 \tag{38}$$

2.10.5. Constraints

Problem constraints are applied in system simulation as follows:

- Power balance constraint:

$$P_{Slack} + \sum_{i=1}^{N} P_{DG_i} = \sum P_{D_i} + P_L \tag{39}$$

- Restrictions on active and reactive power:

$$Q_{DGi}^{min} \le Q_{DGi} \le Q_{DGi}^{max}$$
$$P_{DGi}^{min} \le P_{DGi} \le P_{DGi}^{max} \tag{40}$$

- Losses:

$$\sum Loss_k(withDG) \le \sum Loss_k(withoutDG) \tag{41}$$

- System reliability constraints:

$$\sum SAIDI_k(withDG) \le \sum SAIDI_k(withoutDG)$$
$$\sum SAIFI_k(withDG) \le \sum SAIFI_k(withoutDG) \tag{42}$$
$$\sum AENS_k(withDG) \le \sum AENS_k(withoutDG)$$

- The number of photovoltaic (PV) panels and wind turbines (WT):

$$N_{PV_{min}} \le N_{PV} \le N_{PV_{max}}$$
$$N_{WT_{min}} \le N_{WT} \le N_{WT_{max}} \tag{43}$$

- Voltage and bus current:

$$|V_i|^{min} \le |V_i| \le |V_i|^{max}$$
$$|I_i| \le |I_i|^{max} \tag{44}$$

3. RESULTS AND DISCUSSION

In order to demonstrate the accuracy and precision of the GA-Improved algorithm, the IEEE standard 30-bus network, which is shown in Figure 9, has been studied and evaluated. Taking into account the network losses before installing DG and the resulting voltage drop in the power system, the selected DG capacity for the network is equal to 3.43 MW. Considering that the purchase price of electricity by renewable units to the network in Iran is equal to 0.045 $/kW, the rate of return on equity is equal to 7.6 years during the operation period of the system.

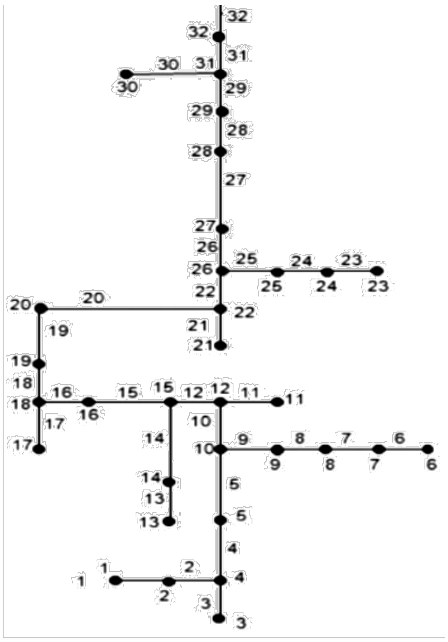

Figure 9. Single-line diagram of the studied network

The convergence process of the proposed algorithm is intended to solve the problem with the objectives and is shown in the form of a single-objective problem in Figure 10.

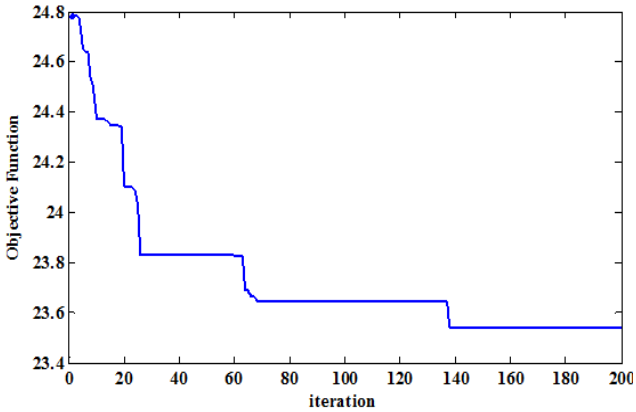

Figure 10. Convergence process of the GA-improved algorithm

The values obtained for system losses before and after DG installation and the rate of improvement of the network voltage profile after DG installation are seen in Figures 11, 12, and 13, respectively.

According to Figure 11, with the placement of DG in bus 8 of the study network, system losses have been significantly reduced compared to the case of no DG installation and have a value equal to 72.48 kW. However, this amount of losses before installing DG had a value of 172.64 kW. The rate of reactive system losses in the two cases before and after the installation of DG is also seen in Figure 12.

According to Figure 12, the reactive loss rate after DG installation has a lower value than the case of no DG installation. According to the results of optimal placement of DG in the desired bus, the system reactive losses from the amount of 126.17 MVAR before installing DG have reached 37.46 MVAR after installing DG in the desired bus. Significant reduction of these losses for the installation of one DG unit with the aim of achieving the least losses is one of the important achievements of this study. Figure 13, which is related to the voltage profile of the studied network, shows the acceptable improvement of the system voltage profile after DG installation.

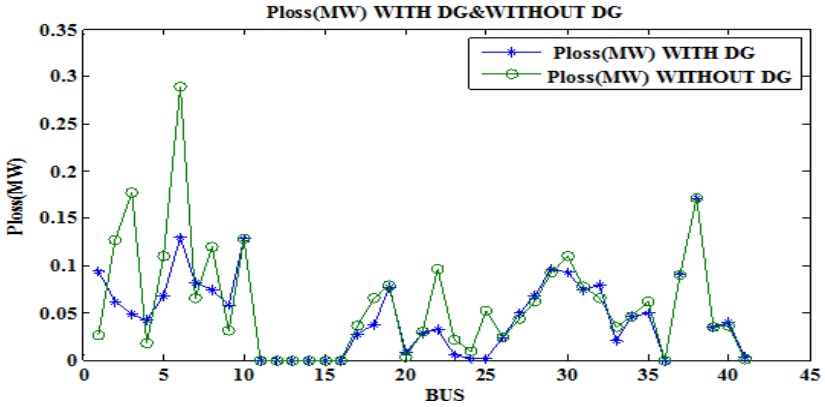

Figure 11. Active network losses before and after DG installation

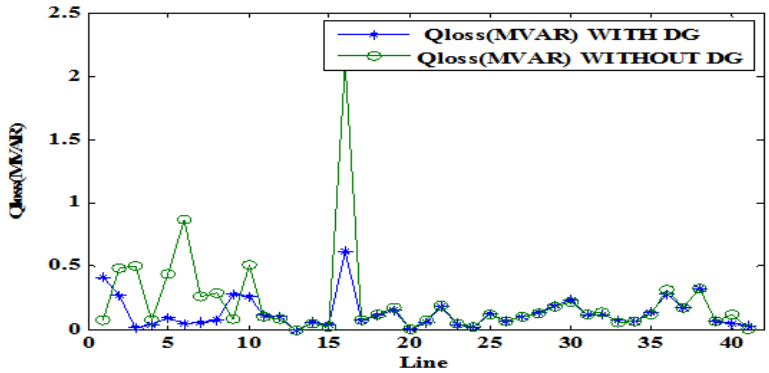

Figure 12. Reactive network losses before and after DG installation

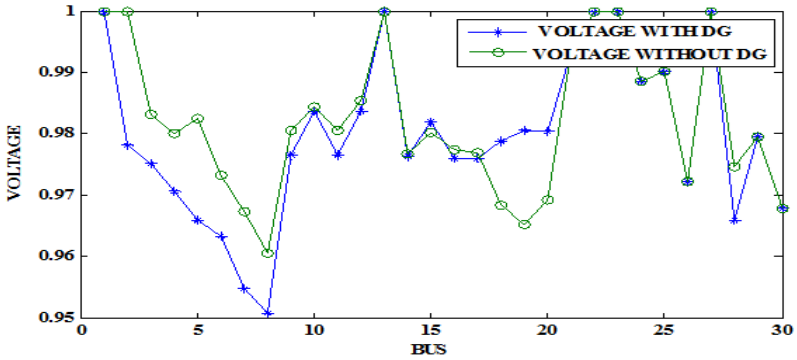

Figure 13. Network voltage profile before and after DG installation

According to Figure 13, the rate of the reduction of voltage profile in the case without using DG has a value equal to 0.7346 P.u, while after installing DG with a capacity of 3.43 MW in the bus 8 of the above network, this index reached 0.9424 P.u.

The results of the system simulation are also presented numerically in Table 2. According to Table 2, the total grid voltage profile improved by 0.2078 (P.u) after DG installation. The optimal reduction of system reliability values according to the values obtained for SAIDI, SAIFI, and AENS indices can be seen in the table. The required capacity of the network for the design and installation of DG is equal to the amount of 3.43 MW, which includes 24 photovoltaic panels, 5 wind turbines, and 11 inverters at a cost of 1.552 M$/MW.

Table 2. Results of the GA-improved algorithm

Parameter	Population size	Bus bar	Total capacity DG	Power losses (kW)	lowest voltage (P.u.)	SAIDI (h/yr.cent)	SAIFI (h/yr.cent)	AENS (kWh/yr)	PV (kW)	WT	Conv. (kW)	NPC (M$/MW)
Without DG	50	-	-	172/64	0.7346	19/8	6/45	328/79	-	-	-	-
With DG	50	8	3/43	72/48	0.9424	4/36	1/04	126/42	24	5	11	1/552

According to the results related to system reliability, the index SAIFI has a value equal to 1.04 times of shutdown during the year and this means that this index, which indicates the average shutdown frequency of the entire network, has a value of 1.04 during the year, which is a very desirable amount in the design of distributed generation systems. It should be noted that the value of this index, as seen in Table 2, had a value of 6.45 times a year without the use of DG. By improving the reliability index of the second system, the SAIDI index was formed and calculated in this research and had an average value of 4.36 hours per year, while this index for the system without the use of DG was calculated and it accounted for 19.8 hours per year, which was a decrease in the indicator of the usefulness and obligation to install DG in the network during the operation period. Then, the third index of the system reliability, AENS is calculated for both cases before and after DG installation and is applied in the table resulting from the system simulation. This loss index after installing DG in the desired bus has a reduction of about 200 kWh during the year and has a value equal to 126.42 kWh per year.

According to the results, the total amount of losses after installing DG was reduced to 72.48 KW. The construction cost of the DG power plant, in this case, was quite smaller than that in previous studies, which was due to the selection of the optimal combination of wind and solar units to ensure the desired load in the study network.

4. CONCLUSIONS

In this research, the location and determination of the optimal capacity of distributed generation units for the IEEE standard network were done by the GA improved algorithm. The high accuracy and precision of the proposed algorithm was one of the main reasons for choosing this algorithm due to the lack of need for many control parameters. The objective function modeling of the problem included power losses, voltage profiles, reliability, DG size, and construction cost of the combined wind and solar combined generation unit in this study. The results of optimization show a 61.23 % reduction of total system losses after DG installation and improvement of system reliability indices, especially the SAIFI, from 6.45 (h/year) to 1.04 (h/year) after installing DG. Reducing the construction cost of DG unit, an optimal increase of network reliability, and significant reduction of power losses were the advantages of choosing the combined wind and solar mode in the studied network. The rate of return on capital was also calculated for the proposed hybrid system in this paper and had a rate of 7.6 years during the operation period of the system. According to the results, the total amount of losses after installing DG was reduced to 72.48 kW. The construction cost of DG power plant, in this case, was quite smaller than that in previous studies due to the selection of the optimal combination of wind and solar units, thus ensuring the desired load in the study network.

5. ACKNOWLEDGEMENT

The authors appreciatively acknowledge the Islamic Azad University of Germi Branch.

NOMENCLATURE

R	Resistance (Ω)
X	Reactance (Ω)
Y	Harmonic
V	Voltage (V)
Q	Reactive power (VA)
P	Active power (kW)
I	Current (A)
λ	Failure rate
N	Number of customers
U	Annual outage time
Ir	Discount rate
T	Temperature (k)
GT	Average daily radiation (W/m^2)
h	Hour

REFERENCES

1. Adebayo, T.S., Coelho, M.F., Onbaşıoğlu, D.Ç., Rjoub, H., Mata, M.N., Carvalho, P.V., Rita, J.X. and Adeshola, I., "Modeling the dynamic linkage between renewable energy consumption, globalization, and environmental degradation in South Korea: Does technological innovation matter?", ***Energies***, Vol. 14, No. 14, (2021), 4265. (https://doi.org/10.3390/en14144265).
2. Khosravi, A., Malekan, M., Pabon, J.J.G., Zhao, X. and Assad, M.E.H., "Design parameter modelling of solar power tower system using adaptive neuro-fuzzy inference system optimized with a combination of genetic algorithm and teaching learning-based optimization algorithm", ***Journal of Cleaner Production***, Vol. 244, (2020), 118904. (https://doi.org/10.1016/j.jclepro.2019.1189).
3. Alayi, R., Zishan, F., Mohkam, M., Hoseinzadeh, S., Memon, S. and Garcia, D.A., "A sustainable energy distribution configuration for microgrids integrated to the national grid using back-to-back converters in a renewable power system", ***Electronics***, Vol. 10, No. 15, (2021), 1826. (https://doi.org/10.3390/electronics10151826).
4. El Haj Assad, M., Ahmadi, M.H., Sadeghzadeh, M., Yassin, A. and Issakhov, A., "Renewable hybrid energy systems using geothermal energy: Hybrid solar thermal–geothermal power plant", ***International Journal of Low-Carbon Technologies***, Vol. 16, No. 2, (2021), 518-530. (https://doi.org/10.1093/ijlct/ctaa084).

5. Sina, M.A. and Adeel, M.A., "Assessment of stand-alone photovoltaic system and mini-grid solar system as solutions to electrification of remote villages in Afghanistan", ***International Journal of Innovative Researchand Scientific Studies***, Vol. 4, No. 2, (2021), 92-99. (https://doi.org/10.53894/ijirss.v4i2.62).
6. Adewole, B.Z., Malomo, B.O., Olatunji, O.P. and Ikobayo, A.O., "Simulation and experimental verification of electrical power output of a microcontroller based solar tracking photovoltaic module", ***International Journal of Sustainable Energy and Environmental Research***, Vol. 9, No. 1, (2020), 34-45. (https://doi.org/10.18488/journal.13.2020.91.34.45).
7. Adebayo, T.S., Rjoub, H., Akinsola, G.D. and Oladipupo, S.D., "The asymmetric effects of renewable energy consumption and trade openness on carbon emissions in Sweden: New evidence from quantile-on-quantile regression approach", ***Environmental Science and Pollution Research***, (2021), 1-12. (https://doi.org/10.1007/s11356-021-15706-4).
8. Ghalandari, M., Ziamolki, A., Mosavi, A., Shamshirband, S., Chau, K.W. and Bornassi, S., "Aeromechanical optimization of first row compressor test stand blades using a hybrid machine learning model of genetic algorithm, artificial neural networks and design of experiments", ***Engineering Applications of Computational Fluid Mechanics***, Vol. 13, No. 1, (2019), 892-904. (https://doi.org/10.1080/19942060.2019.1649196).
9. Alayi, R., Zishan, F., Seyednouri, S.R., Kumar, R., Ahmadi, M.H. and Sharifpur, M., "Optimal load frequency control of island microgrids via a PID controller in the presence of wind turbine and PV", ***Sustainability***, Vol. 13, No. 19, (2021), 10728. (https://doi.org/10.3390/su131910728).
10. Kefif, N., Melzi, B., Hashemian, M., El Haj Assad, M. and Hoseinzadeh, S., "Feasibility and optimal operation of micro energy hybrid system (hydro/wind) in the rural valley region", ***International Journal of Low-Carbon Technologies***, Vol. 17, (2022), 58-68. (https://doi.org/10.1093/ijlct/ctab081).
11. Mostafaeipour, A., Saidi Mehrabad, M., Qolipour, M., Basirati, M., Rezaei, M. and Golmohammadi, A.M., "Ranking locations based on hydrogen production from geothermal in Iran using the Fuzzy Moora hybrid approach and expanded entropy weighting method", ***Journal of Renewable Energy and Environment (JREE)***, Vol. 4, No. 4, (2017), 9-21. (https://dx.doi.org/10.30501/jree.2017.88328).
12. Hsu, C.C., Zhang, Y., Ch, P., Aqdas, R., Chupradit, S. and Nawaz, A., "A step towards sustainable environment in China: The role of eco-innovation renewable energy and environmental taxes", ***Journal of Environmental Management***, Vol. 299, (2021), 113609. (https://doi.org/10.1016/j.jenvman.2021.113609).
13. AlShabi, M., Ghenai, C., Bettayeb, M., Ahmad, F.F. and El Haj Assad, M., "Multi-group grey wolf optimizer (MG-GWO) for estimating photovoltaic solar cell model", ***Journal of Thermal Analysis and Calorimetry***, Vol. 144, No. 5, (2021), 1655-1670. (https://doi.org/10.1007/s10973-020-09895-2).
14. Mughal, N., Arif, A., Jain, V., Chupradit, S., Shabbir, M.S., Ramos-Meza, C.S. and Zhanbayev, R., "The role of technological innovation in environmental pollution, energy consumption and sustainable economic growth: Evidence from South Asian economies", ***Energy Strategy Reviews***, Vol. 39, (2022), 100745. (https://doi.org/10.1016/j.esr.2021.100745).
15. Fu, L., Liu, B., Meng, K. and Dong, Z.Y., "Optimal restoration of an unbalanced distribution system into multiple microgrids considering three-phase demand-side management", ***IEEE Transactions on Power Systems***, Vol. 36, No. 2, (2020), 1350-1361. (https://doi.org/10.1109/TPWRS.2020.3015384).
16. Makkiabadi, M., Hoseinzadeh, S., Mohammadi, M., Nowdeh, S.A., Bayati, S., Jafaraghaei, U., Mirkiai, S.M. and El Haj Assad, M., "Energy feasibility of hybrid PV/wind systems with electricity generation assessment under Iran environment", ***Applied Solar Energy***, Vol. 56, No. 6, (2020), 517-525. (https://doi.org/10.3103/S0003701X20060079).
17. Abbas, A.S., El-Sehiemy, R.A., El-Ela, A., Ali, E.S., Mahmoud, K., Lehtonen, M. and Darwish, M.M., "Optimal harmonic mitigation in distribution systems with inverter based distributed generation", ***Applied Sciences***, Vol. 11, No. 2, (2021), 774. (https://doi.org/10.3390/app11020774).
18. Marquez Alcaide, A., Monopoli, V.G., Wang, X., Leon, J.I., Buticchi, G., Vazquez, S., Liserre, M. and Franquelo, L.G., "Common-mode voltage harmonic reduction in variable speed drives applying a variable-angle carrier phase-displacement PWM method", ***Energies***, Vol. 14, No. 10, (2021), 2929. (https://doi.org/10.3390/en14102929).
19. Liu, Y., Xu, W., Long, T. and Blaabjerg, F., "An improved rotor speed observer for standalone brushless doubly-fed induction generator under unbalanced and nonlinear loads", ***IEEE Transactions on Power Electronics***, Vol. 35, No. 1, (2019), 775-788. (https://doi.org/10.1109/TPEL.2019.2915360).
20. Manito, A., Bezerra, U., Tostes, M., Matos, E., Carvalho, C. and Soares, T., "Evaluating harmonic distortions on grid voltages due to multiple nonlinear loads using artificial neural networks", ***Energies***, Vol. 11, No. 12, (2018), 3303. (https://doi.org/10.3390/en11123303).
21. Norozpour Niazi, A., Vasegh, N. and Motie Birjandi, A.A., "To study unplanned islanding transient response of microgrid by implementing MSOG and SRF-PLL based hierarchical control in the presence of non-linear loads", ***IET Renewable Power Generation***, Vol. 14, No. 5, (2020), 881-890. (https://doi.org/10.1049/iet-rpg.2019.0506).
22. Laffont, A., Pascaud, R., Callegari, T., Liard, L., Pascal, O. and Adam, J.P., "A harmonic oscillator model to study the intensification of microwave radiation by a subwavelength uniform plasma discharge", ***Physics of Plasmas***, Vol. 28, No. 3, (2021), 033503. (https://doi.org/10.1063/5.0038640).
23. Pan, C. and Su, H., "Research on excitation current and vibration characteristics of DC biased transformer", ***CSEE Journal of Power and Energy Systems***, (2019). (https://doi.org/10.17775/CSEEJPES.2019.00410).
24. Jamali-Abnavi, A., Hashemi-Dezaki, H., Ahmadi, A., Mahdavimanesh, E. and Tavakoli, M.J., "Harmonic-based thermal analysis of electric arc furnace's power cables considering even current harmonics, forced convection, operational scheduling, and environmental conditions", ***International Journal of Thermal Sciences***, Vol. 170, (2021), 107135. (https://doi.org/10.1016/j.ijthermalsci.2021.107135).
25. Hemmati, M., Mohammadi-Ivatloo, B., Abapour, M. and Anvari-Moghaddam, A., "Optimal chance-constrained scheduling of reconfigurable microgrids considering islanding operation constraints", ***IEEE Systems Journal***, Vol. 14, No. 4, (2020), 5340-5349. (https://doi.org/10.1109/JSYST.2020.2964637).
26. Das, C.K., Bass, O., Kothapalli, G., Mahmoud, T.S. and Habibi, D., "Overview of energy storage systems in distribution networks: Placement, sizing, operation, and power quality", ***Renewable and Sustainable Energy Reviews***, Vol. 91, (2018), 1205-1230. (https://doi.org/10.1016/j.rser.2018.03.068).
27. Narimani, M. and Hosseinian, H., "Investigation of harmonic effects in locational marginal pricing and developing a framework for LMP calculation", ***Scientia Iranica***, (2020). (https://dx.doi.org/10.24200/sci.2020.54477.3776).
28. Das, T.K. and Chatterjee, S., "Multi-spurious harmonics suppression in folded hairpin line bandpass filter by meander spur-line", ***International Journal of RF and Microwave Computer-Aided Engineering***, Vol. 31, No. 11, (2021), e22858. (https://doi.org/10.1002/mmce.22858).
29. Gu, Z., Malik, H.A., Chupradit, S., Albasher, G., Borisov, V. and Murtaza, N., "Green supply chain management with sustainable economic growth by CS-ARDL technique: Perspective to blockchain technology", ***Frontiers in Public Health***, 2391. (https://doi.org/10.3389%2Ffpubh.2021.818614).
30. Alayi, R., Jahangiri, M., Guerrero, J.W.G., Akhmadeev, R., Shichiyakh, R.A. and Zanghaneh, S.A., "Modelling and reviewing the reliability and multi-objective optimization of wind-turbine system and photovoltaic panel with intelligent algorithms", ***Clean Energy***, Vol. 5, No. 4, (2021), 713-730. (https://doi.org/10.1093/ce/zkab041).